Toomla, Sander; Lestinen, Sami; Kilpeläinen, Simo; Leppä, Lauri; Kosonen, Risto; Kurnitski, Jarek

Experimental investigation of air distribution and ventilation efficiency in an ice rink arena

Published in:
International Journal of Ventilation

DOI:
10.1080/14733315.2018.1437881

Published: 03/07/2019

Document Version
Peer-reviewed accepted author manuscript, also known as Final accepted manuscript or Post-print

Please cite the original version:
Toomla, S., Lestinen, S., Kilpeläinen, S., Leppä, L., Kosonen, R., & Kurnitski, J. (2019). Experimental investigation of air distribution and ventilation efficiency in an ice rink arena. *International Journal of Ventilation*, *18*(3), 187-203. https://doi.org/10.1080/14733315.2018.1437881

Experimental investigation of air distribution and ventilation efficiency in an ice rink arena

Sander Toomla[a], Sami Lestinen[b], Simo Kilpeläinen[b], Lauri Leppä[a], Risto Kosonen[b], Jarek Kurnitski[a,c]

[a]Department of Civil Engineering, School of Engineering, Aalto University, Espoo, Finland; [b]Department of Mechanical Engineering, School of Engineering, Aalto University, Espoo, Finland; [c]Department of Civil Engineering and Architecture, School of Engineering, Tallinn University of Technology

Keywords: Air distribution; Ventilation efficiency; Ice rink arena; Stratification; Measurement

Abstract

This study presents extensive experimental measurements in a modern Finnish ice rink arena including temperature, relative humidity, carbon dioxide, air speed, air flow and pressure difference measurements in addition to smoke tests. Furthermore, the air exchange rate (ACH), air-exchange efficiency, and mixing factor were calculated. The main aim was to determine ventilation effectiveness, vertical stratification of the air and how commonly re-circulation can be used in a modern ice rink arena representing common practice. Results show that re-circulation of return air was virtually continuous and in normal operating conditions the outdoor air fraction of the supply air was only 3.7 % corresponding to ACH of 0.03 1/h. The ceiling distributed mixing ventilation was not able to mix the whole volume sufficiently, leading to two imperfectly mixed zones with an average air-exchange efficiency of 39 % in the lower zone, corresponding to a mixing factor of 1.7.

Introduction

Indoor ice arenas present unique and challenging environments for the design and execution of efficient ventilation systems. The required indoor environment, including the ice pad, generate complex phenomena that lead to complicated air movement, mixing and indoor air conditions.

The importance of ventilation and dehumidification is acknowledged in the guidelines of IIHF

Contact: Sander Toomla: sander.toomla@aalto.fi

(2016) although a far more detailed approach is needed to ensure the functionality and efficiency of these systems in practice. The ice rink arenas are large enclosures where complete mixing of the air is hard to achieve especially when the supply and extract points are located near the ceiling. Instead, non-uniform conditions can be promoted to use the non-occupied zone as storage for rising heat and contaminants (Heiselberg et al., 1998).

Experimental measurements of ventilation performance and air movement in the ice arenas require numerous measurement points throughout the space and when tracer gas measurements are used, the needed amount and adequate distribution of the tracer may become problematic (Liddament et al., 1998). Only a few publications rely mostly on extensive experimental measurements of ice arenas although many studies present limited experimental data for validation. Yang et al. (2000) presented some physical characteristics, air flow rates and air exchange rates of ten ice rinks arenas located in the area of Great Boston and Halifax, Nova Scotia. Later Yang et al. (2002) presented a tracer-gas based experimental method that can be used for both experimental evaluation and CFD validation in large buildings, including ice rink arenas. A study by Ouzzane et al. (2006) presents the measurements performed in a Canadian indoor ice arena and also describes the building design in detail.

The indoor conditions and air movement inside the ice rink arenas have mostly been studied via computational fluid dynamics (CFD). Yang et al. (2001) presented and validated the use of a CFD model in an ice rink arena that sufficiently predicted the air velocity, air temperature and contaminant concentrations. Bellache et al. (2005) presented a 2D CFD model of an air heated ice rink arena that predicted velocity, temperature and absolute humidity of the indoor air. This study also included calculated heat fluxes toward the ice due to convection, condensation and radiation. Bellache et al. (2006) improved the previous study to include transient phenomena, heat transfer through the ground and heat gains caused by lights, resurfacing and pump work. Omri & Galanis (2010) presented a 3D CFD model to study the flow and temperature fields of a radiator heated ice rink arena in both steady and transient states. This study was recently extended by Omri et al. (2016) by calculating and analysing the flow and temperature fields in the same ice rink over a 24-hour period for time dependent outdoor conditions with variable temperatures and flow rates of the ventilation air. Lestinen et al. (2016) showed that CFD can also be used to explore thermal conditions, indoor air quality, airflow patterns and air distribution in larger multipurpose arenas. Although CFD is the most common approach to study the indoor air conditions and movement in ice rink arenas Daoud et al., (2008) reached a good agreement with published CFD results and experimental data in their numerical study which constitutes as an alternative to CFD modelling.

The lack of extensive experimental studies also reflects on the validation of CFD models, as the models need to be validated with corresponding experimental data before the CFD can be used for further studies (Liu et al., 2013; Chen & Srebric, 2002).

There are two main shortcomings in the previously mentioned studies about ice rink arenas. Firstly, the presented ventilation design and air distribution are most commonly simplistic and mainly do not consider variable air flow rates and re-circulation of the air. These factors of air handling combined with more sophisticated air distribution systems must be taken into account when studying modern ice rink arenas. Secondly, although CFD simulations show relatively good agreement with measured data in general, the numerical results tend to underestimate the cooling effects of the ice near its surface, which is crucial when the indoor environment of the occupied zone is studied.

This study presents full-scale experimental data of the indoor air conditions and the ventilation performance in a modern Finnish ice rink arena. Extensive experimental measurements include temperature, relative humidity, carbon dioxide, air speed, air flow and pressure difference measurements in addition to smoke tests. Furthermore, the air exchange rate (ACH), air-exchange efficiency ε_a, (Mundt, et al. 2004) and mixing factor β (Etheridge & Sandberg, 1996) are calculated.

The novelty of this study is the assessment of efficiency and performance of the commonly used mixing ventilation in a modern case study ice rink arena. In addition, the effects of heavy air re-circulation on the indoor environment are discussed and the vertical stratification profiles of this study are compared to other publications.

The study improves the knowledge on indoor airflows and their behaviour in ice arenas. The results can be utilized to describe more realistic design assumptions as well as for alternative ventilation and air conditioning design and for the validation of CFD models to study the performance of this particular (or similar) arena with altered ventilation designs. More widely, the results can also be utilized for energy calculation methods development for ice rink arenas.

Methods

Case study presentation

In this study, the performance of a typical Finnish ice rink arena was measured. The studied ice arenas hall volume is a 13000 m^3 uniform airspace with minimum 5 m of free height above the ice rink. The total floor area of the hall space is 1833 m^2 and the ice pad area is 1508m^2 (58m*26m). The ice is maintained with an electrical resurfacing machine. There is a spectator balcony for 60 people (77 m^2) 3 m above ice level. Dressing and storage rooms and a cafeteria are located on one long wall in two stories. Only the hall space is considered in this study. The inner surfaces of the ice arenas hall are concrete floor, painted (white) steel cassette wall structure and corrugated steel ceiling.

The ice arena is heated and ventilated via mechanical mixing ventilation. The basic principles of the air handling unit (AHU) are presented in Fig. 1. The system is equipped with modern automation, which enables variable air volume (VAV) operation, monitoring and ventilation control strategy. The demand based air flow rate (up to 4 m^3/s) is adjusted by the indoor air setpoints. Key features of this AHU are the use of re-circulation air, heat recovery and dehumidification. Whenever possible, the system utilizes the maximum amount of re-circulation air which reduces the needs for dehumidification and heating or cooling. The positioning and utilization of heat exchanger and the dehumidification coil further reduce the need for cooling energy. Outdoor air is used only when the indoor carbon dioxide (CO_2) setpoint is exceeded. A crucial characteristic of the AHU in operation was that the exhaust fan was off and the outdoor and exhaust air dampers were fully closed for the vast majority of the time. As a result, the whole AHU was underpressurized by the supply fan.

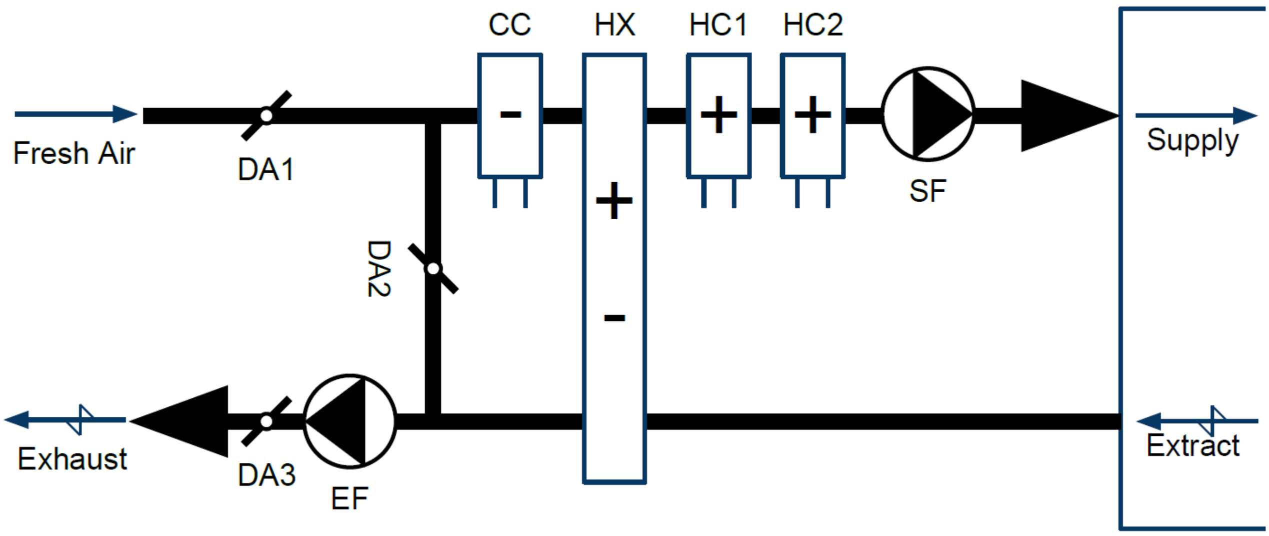

Figure 1. Layout of the AHU serving the hall space of the studied ice rink arena. In typical operation the extract air is fully recirculated to the cooling coil (CC), heat recovery (HX), and reheated in two steps (HC1 & HC2). Dampers DA1 and DA3 are closed, and DA2 is open. Supply fan (SF) is always on and the exhaust fan (EF) was seldomly used together with changing over the dampers positions for very short periods if the CO_2 concentration exceeded the limit value of 1000 ppm in the occupation zone.

Air distribution inside the hall space was executed with 11 high-momentum air jets located near the ceiling and directed toward the ice. The locations of the supply air nozzles and extract outlets are shown in Fig. 2a. The nozzle of the high-momentum supply air jet is shown in Fig. 2b.

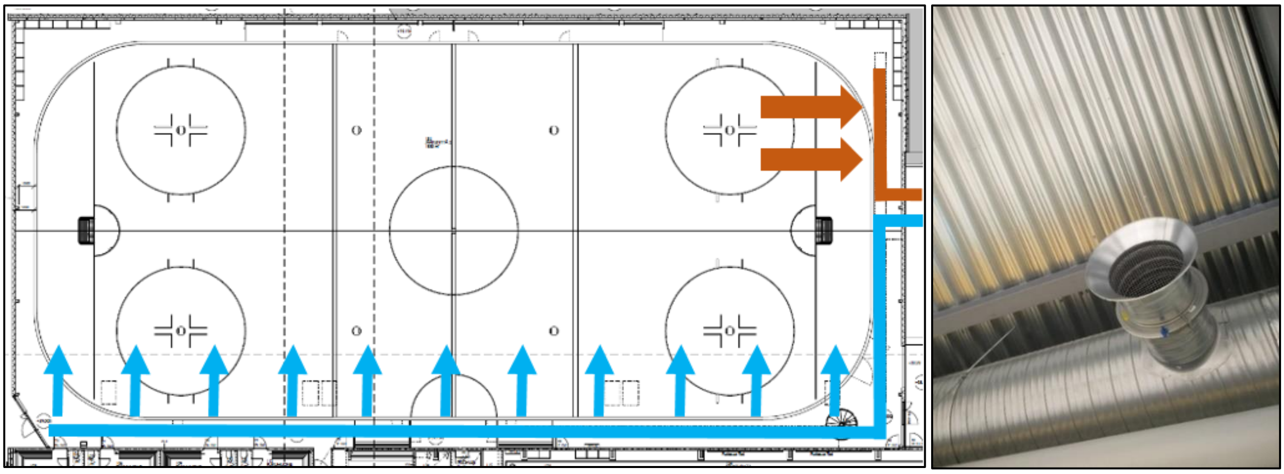

Figure 2 a) The location of the supply air nozzles and extract points. b) A supply air nozzle (Ø315 mm) adjusted by a Halton PRA damper.

Measurements

The following measurements were conducted in the ice rink arena:

- Total supply air flow rates (3 – 12.5.2016)
- Total exhaust air flow rates (3 – 12.5.2016)
- Temperature, relative humidity and carbon dioxide (CO_2) concentration of supply air (leaving the air handling unit) (3 – 12.5.2016)
- Temperature, relative humidity, carbon dioxide (CO_2) concentration and carbon monoxide (CO) concentration of return air (3 – 12.5.2016)
- Air speeds in several locations (3 & 4.5.2016)
- Smoke test (3.5.2016)
- Indoor air temperature, relative humidity and carbon dioxide (CO_2) concentration in several locations near walls (3 – 12.5.2016)

- Outdoor temperature and relative humidity on site (3 – 12.5.2016)
- Indoor air stratification above the ice pad in several locations (4.5.216)
- Pressure difference over building envelope in two locations (4 – 12.5.2016)

From the two-week measurement period, we mainly concentrate on the May 4th 2016 since some measurements were conducted only on that day. This one-day timeframe is also detailed enough to show the fluctuation of many measured parameters that were observed throughout the measurement period.

The following devices were used for measurements. The air flow rates were measured with two Swema 3000md (Swema AB, 2017). The conditions of supply and indoor air (near walls) were measured with seven Rotronic CL11 devices (Rotronic AG, 2017). Return air measurements were conducted with a Delta Ohm HD21AB17 device (Delta OHM S.r.L., 2017). Outdoor air conditions and air stratification inside the ice rink were measured with Thermadata HTD devices (ETI Ltd, 2017). It should be noted that the structure of these devices is such that the measurement probe is protected against direct radiation. The airflow field was investigated using three wireless Sensoanemo hot-sphere anemometers (Sensor Electronic, 2017) and smoke visualization. Measurement accuracy of all the devices used in this study are presented in Table 1.

Temperature, relative humidity and CO_2 concentration of indoor air was logged in six different locations illustrated in Fig. 3. Five points were located 2 meters above ice level and 20 cm away from walls. One point (6) was located on the spectator balcony about 5.2 m above ice level and over 1 m away from walls and ceiling. All of the points were located outside the rink to enable long term measurements. Readings were recorded every 5 minutes. Outdoor air temperature and relative humidity were logged in 5 minute intervals.

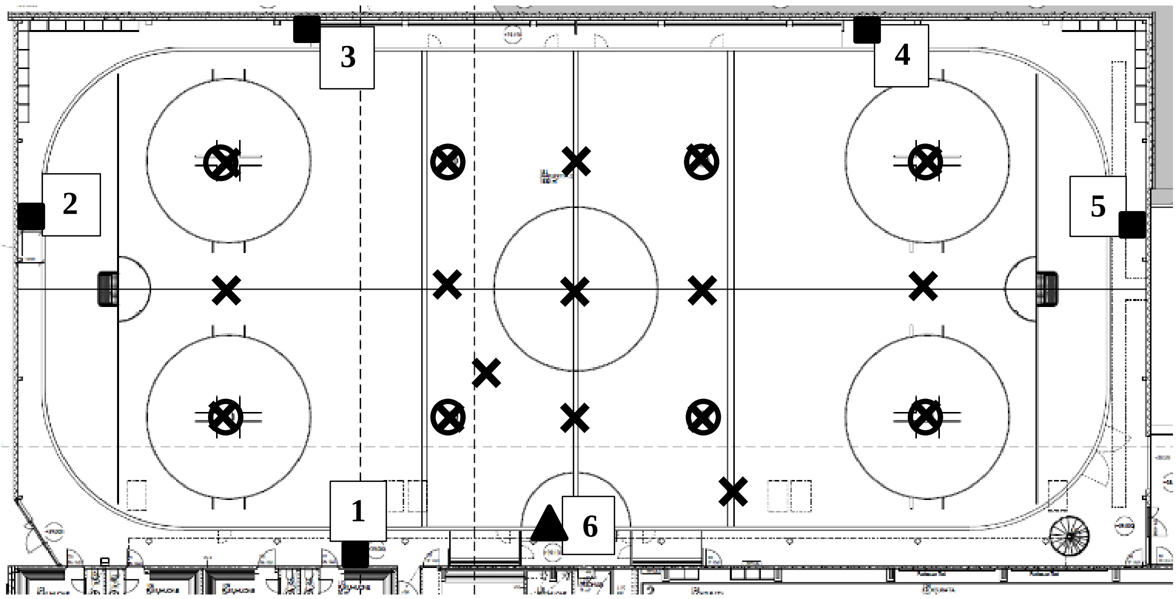

Figure 3. Measurement locations inside the ice rink arena. Indoor air conditions near walls at occupation zone and at spectator balcony marked with squares and a triangle respectively. Air flow velocity measurement point on ice presented by X:s. Temperature gradient measurement points shown by circles. Numbering refers to the indoor air measurement points only.

Indoor air vertical stratification was measured at the heights of ~0.01m (device laying on ice), 0.1 m, 0.25 m, 0.5 m, 1 m, 1.5 m, 2 m, 3 m, 4 m, 5 m. Measurements were conducted in eight locations on ice which are presented in Fig. 3. Recording interval of these measurements was 6 seconds. The measurements were carried out in cycles of minimum 10 minutes in order to allow the measurement devices to set in changed conditions. Before starting the measurements, the devices were erect and kept in place on ice for two hours to ensure a suitable starting point for the measurements.

The air speed measurements were conducted in total 17 locations illustrated in Fig. 3. Measurement heights were 3 m, 3.7 m and 4.3 m above ice surface. At lower heights the air movement was not measured due to the observation during smoke tests that the air in lower regions was found to be essentially stagnant.

Table 1. Measurement accuracy of devices used in this study.

Device	**Measured parameters**	**Measurement accuracy**
Swema 3000 md	Pressure difference (air flow rate)	±0.3% of reading, minimum ±0.3 Pa, 2…49m/s
Rotronic CL11	Temperature, Relative humidity, CO_2 concentration	±30 ppm ±5 % of the measured value, <2.5 % RH (10…90 %RH), ±0.3°K
Delta Ohm HD21AB17	Temperature, Relative humidity, CO_2 concentration, CO concentration, atmosphere pressure	CO_2: ±50ppm +3% of measurement, CO: ±3ppm+3% of measurement, RH: ±2%RH at 10…90% ±2.5%RH otherwise, T: ±0.2 °C ± 0.15% of measurement
Thermadata HTD	Temperature, Relative humidity	T: ±0.5°C (0…+45°C) ±1°C(-20…+70 °C) ±1.5°C (+70…+85 °C) RH: ±2%Rh at +25°C (10…90%Rh)
KIMO CP 101	Pressure difference	±1.5% of reading ±3 Pa
Sensor electronic SensoAnemo 5100SF	Air velocity, Temperature	Air speed: Range 0.05…5 m/s, ±0.02 m/s ±0.015·v_{meas} Temperature: Range −10…50°C ±0.2°C

Outdoor air flow rate and air change effectiveness evaluation

The outdoor air exchange rate (ACH) in the ice arena was calculated similarly to a study by van Hooff & Blocken (2012) using equation (1) by ASHRAE (2013) for tracer gas decay. The ACH was calculated during a night-time period when the hall was empty and the total supply air flow rate, consisting of outdoor and re-circulated air, was constant. For other time periods the outdoor air flow rate was estimated to be proportional to the total supply air flow rate resulting higher outdoor air flow rates during higher supply air flow rates and vice versa. This estimation is consistent with the observation that the supply air fan underpressurized the AHU and thus the leakage of the outdoor air through dampers can be estimated to the proportional to the underpressure created by the supply air fan.

$$ACH = \frac{\ln(C_0) - \ln(C_1)}{\tau_1 - \tau_0} \quad (1)$$

Where C_0 is the CO_2 concentration at time 0 (τ_0) [ppm] and C_1 is the CO_2 concentration at time τ_1 [ppm]. ACH [h^{-1}].

For the upper and lower air zones described in Results, we use the following evaluations. We evaluate the air-exchange efficiency ε_a [%] with the following equation (2) (Mundt et al., 2004):

$$\varepsilon_a = \frac{\tau_n}{\bar{\tau}_r} * 100 = \frac{\tau_n}{2 * \langle\bar{\tau}\rangle} * 100 \quad (2)$$

Where τ_n is the nominal time constant [h], $\bar{\tau}_r$ is the actual air change time and $\langle\bar{\tau}\rangle$ is the mean age of air [h]. For the whole studied volume, the nominal time constant τ_n [h] can be expressed as:

$$\tau_n = \frac{V}{q} \quad (3)$$

Where V is the volume of the space [m^3] and q is the air flow rate [m^3/h].

The short-circuiting of supply air was evident according to the measurements of CO_2 concentrations reported and further discussed in the Results. To assess the mixing in the two air zones found in the smoke tests we rely on the well-established results of Etheridge & Sandberg (1996). When two air zones are formed so that the (lower) occupation zone is ventilated only through mixing with the upper zone where supply and extract are located, the mean age of air $\langle\bar{\tau}\rangle$ in the two zones can be expressed as (Etheridge & Sandberg, 1996):

$$\langle\bar{\tau}\rangle_{upper\ zone} = \tau_n \quad (4)$$

$$\langle\bar{\tau}\rangle_{occupied\ zone} = \frac{(1+2\beta)}{2\beta} * \tau_n \quad (5)$$

Where β is the mixing factor between the two zones. In this case the upper zone is assumed to be perfectly mixed.

The mixing factor β is calculated based on the Euler's method (equation 6) and air zones contaminant concentration mass balance. In this study the contaminant is the CO_2 concentration. For the change rate of contaminant concentration with respect to time we assume that the time steps taken are so short that the change rate can be simplified.

$$C_{t+1} = C_t + \frac{dC}{dt} * \Delta t \ \approx C_t + \frac{\Delta C}{\Delta t} * \Delta t \quad (6)$$

Where C_{t+1} is the concentration at timestep n+1 [ppm], C_t is the concentration at timestep n [ppm], $\frac{dC}{dt}$ describes the change rate in the concentration in time [ppm/s] and Δt is the timestep taken between timesteps n and n+1 [s].

The rate of change for the contaminant can also be expressed via mass balance of the contaminant in the studied zone. The zoning used can be seen from Fig. 12. Thus for the situation at hand a mass balance equation for the upper zone of the ice arena can be formed as follows.

$$VdC_{upper} = \beta * q * C_{lower} * dt - \beta * q * C_{upper} * dt + q * C_s * dt - q * C_{upper} * dt \quad (7)$$

Where V is the volume of the studied zone [m^3], C_{upper} is the CO_2 concentration of the studied, upper zone [ppm], β is the mixing factor [-], q is the air flow rate [m^3/s], C_{lower} is the CO_2

concentration of the zone beneath the studied zone [ppm] and C_s is the CO_2 concentration of the supply air [ppm].

In the equation (7), the contaminant production in the upper zone is assumed to be zero. Also the contaminant production in the lower, occupation zone is assumed to be fully mixed into the lower zone before being mixed to the upper zone. Furthermore, the exfiltration was neglected as only 1.7 Pa positive pressure was measured in the building with respect to outdoor air and the transit of the resurfacing machine in and out of the arena only required the external door to be opened for couple of minutes at a time. The compensating infiltration airflow was assumed to be drawn in through the AHU and is thus taken into account in the supply air concentration. In addition, no absorption of the contaminant was assumed.

The mass balance equation can be rewritten to express the change rate of the CO_2 concentration to form the following equation.

$$\frac{dC}{dt} = q * \frac{\beta * (C_2 - C) + (C_s - C)}{V} \quad (8)$$

This equation can now be inserted into the Euler's equation to solve the mixing factor β with equation (9) where the subscripts t and t+1 represent the consecutive timesteps.

$$\beta = \frac{C_t * V - C_{t+1} * V + C_{s,t} * q * \Delta t - C_t * q * \Delta t}{C_t * q * \Delta t - C_{2,t} * q * \Delta t} \quad (9)$$

The results of the mixing factor β are also crosschecked by using the Euler's equation once again with constant values of the β, CO_2 gain and air flow rate. These results are calculated with given measured CO_2 concentrations of the supply air and compared to the measured indoor CO_2 concentrations.

Results

During the measurements, the outdoor air conditions were varying. The temperature of the outdoor air fluctuated between ~0 – 28 °C with an average of 14.7 °C. Strong fluctuation was mostly caused by the cloudless sky. The relative humidity of the outdoor air varied between ~16 – 83 % with an average of 43.5 % and the absolute humidity varied between 2.3 – 7.1 $g/kg_{d.a.}$ with an average of 4.1 $g/kg_{d.a.}$.

Air distribution and air velocity

Two air zones were found inside the ice rink with extensive smoke tests. Based on several smoke extractions at different locations and hights on the ice pad and studing the video material the air zones were identified. The lower zone was found to form from the ice sheet up to the height of 3 m and correspondigny the upper zone was identified from the height of 3 m up to the ceiling. The air in the lower zone was essentially stagnant as illustrated in Fig. 4. The air in the upper zone was clearly mixed more sufficiently and smoke released into this zone traveled towards the extraction point while noticable vortexes formed near the supply air jets.

Figure 4. Stagnant smoke up to the height of 3 m approximately 2 minutes after the smoke was released at the location of the smoke generator.

The effect of ice-skaters was not present during the smoke tests. It is evident that users mix the stagnant air inside the rink to some extent but the effect will stay in the lower zone. During the smoke tests moving/running through the smoke did not cause significant mixing of the air, which indicates that the air should be mixed efficiently via ventilation to ensure good indoor air conditions.

The flow field in the ice arena was fluctuating as shown in Fig. 5. However, the air was rather quiescent in the ice rink from the ice sheet up to the height of 3 m as showed by the smoke tests described previously. The indoor air was moving due to the supply air jets and coincident forces that have an effect on the flow field. It seems that indoor air motion was increased towards the upper region and the exhaust-end region as shown in Fig. 5. However, the indoor air was moving rather slowly throughout the ice arena, except near the supply air jets. Consequently, the air speed level was slightly higher at the air distribution side than in the middle or in the opposite side of the arena as shown in Fig. 5. However, the air speed levels were varying on those locations.

In detail, the average air speed level was 0.09 m/s at the height of 3 m. The air speed range in turn was from 0 m/s to 0.26 m/s and the standard deviation was 0.05 m/s with 0.5 Hz measuring frequency over the 3 min interval. At the height of 3.7 m, the average air speed level was 33% higher. The average air speed was 0.12 m/s and the range was up to 0.43 m/s. The standard deviation was 0.07 m/s. At the height of 4.3 m, the average air speed was still increasing 12%, hence the average air speed level was 49% greater than at the height of 3 m. Consequently, the average air speed at 4.3 m was 0.13 m/s and the measured range was up to 0.57 m/s with the standard deviation of 0.08 m/s.

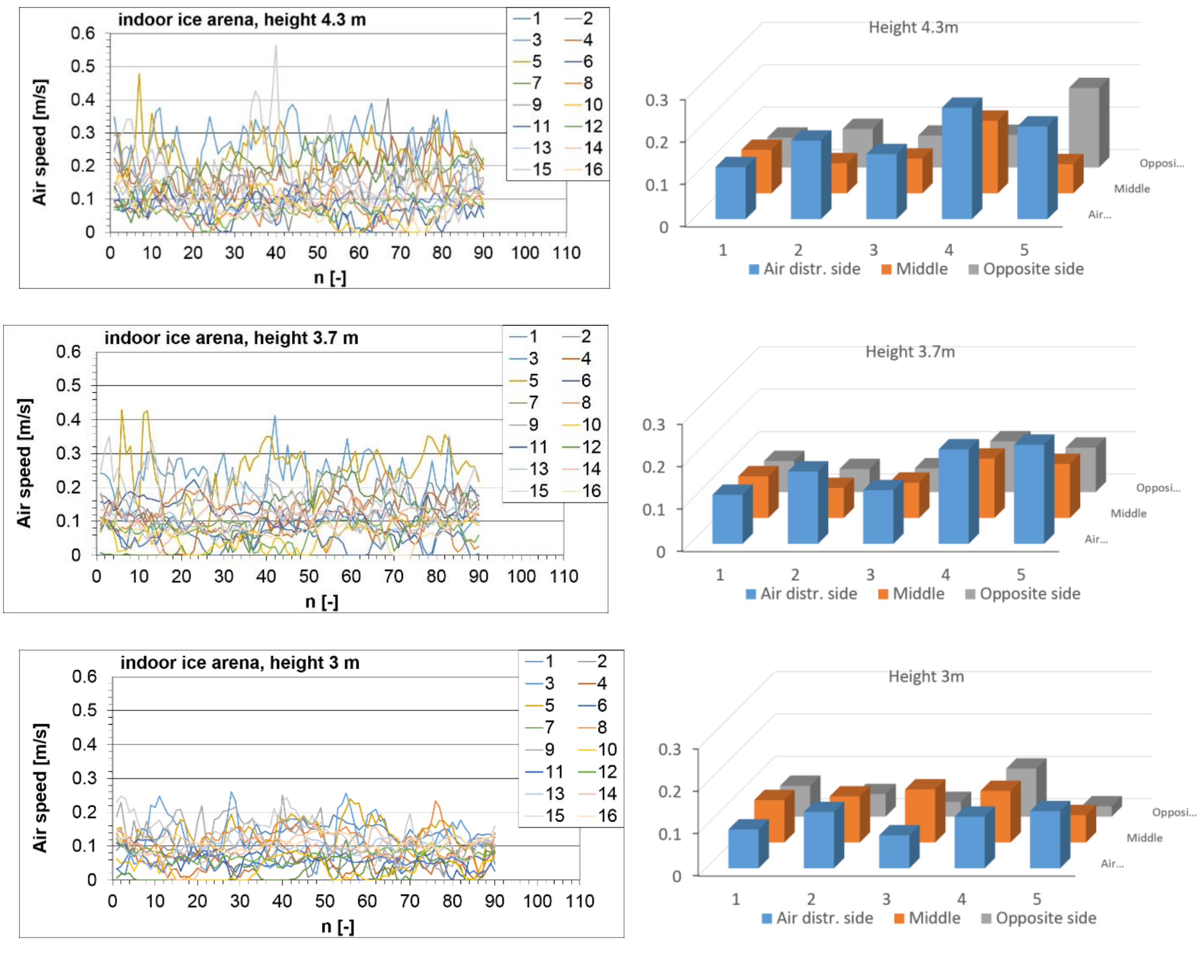

Figure 5. The air speed fluctuation at the height of 3 m, 3.7 m and 4.3 m.

CO_2 concentrations, air exchange rate, temperature and relative humidity

All measured CO_2 concentrations strongly followed the same profile, which indicates high re-circulation of air. As shown in Fig. 6, the concentrations never reach steady state conditions and the supply air concentration fluctuates alongside with indoor air measurements. Substantial outdoor air intake was observed only on two occasions during the weekend of the measurement period when indoor air CO_2 concentrations were elevated beyond the control system setpoint. As the ice was maintained with an electrical resurfacing machine the carbon monoxide level of the extract air was constantly 0 ppm throughout the measurement period.

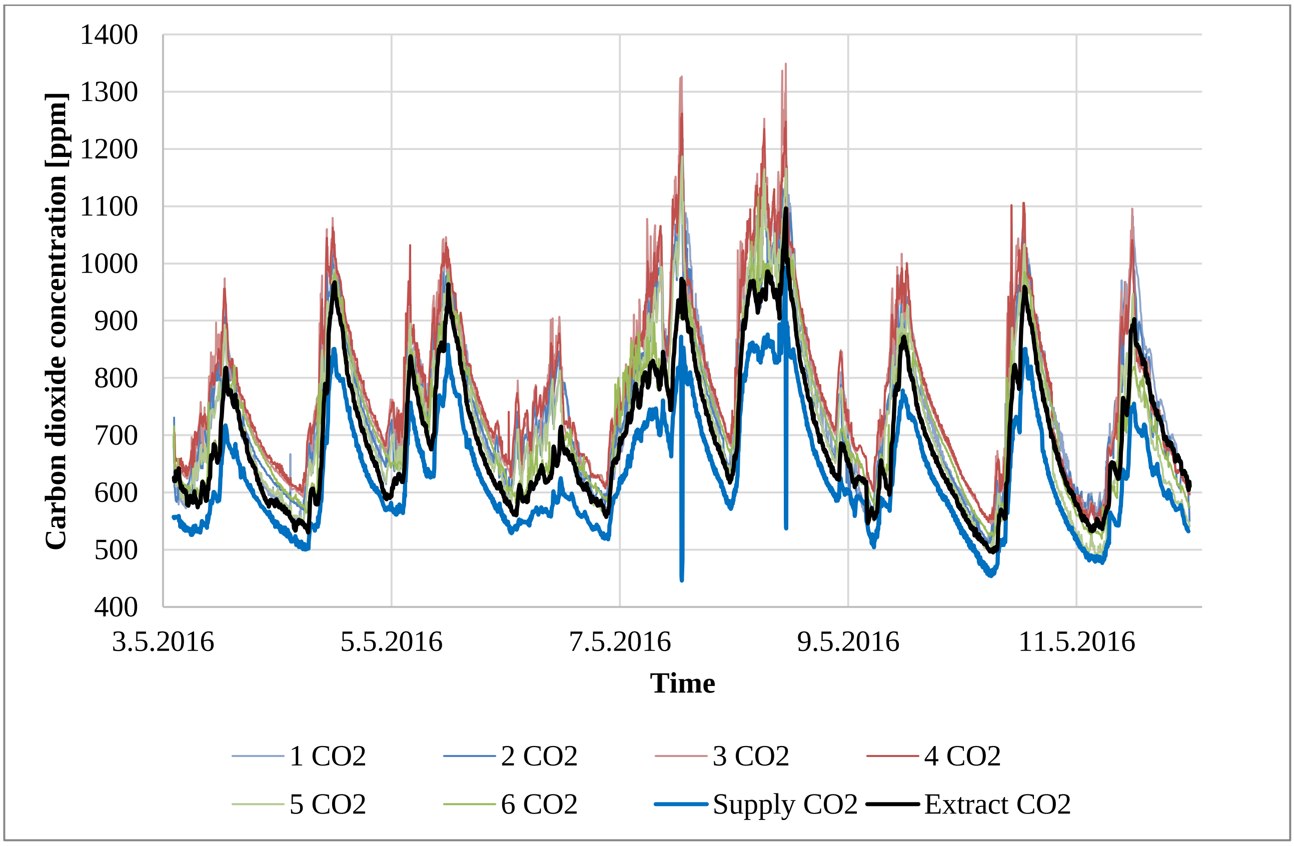

Figure 6. Carbon dioxide concentrations of the indoor ice rink arena.

All of the indoor air CO_2 concentrations follow the same profile and peak at the end of the last training session. After the users leave, the concentration starts to decay until the users occupy the space the next day. This shows that the large air-volume of the ice rink acts as a buffer that slows down the alteration of CO_2 concentration. The measured concentration levels were below 1200 ppm for the majority of the time but some measurements did exceed that value briefly, especially during the weekend when more people occupied the space. CO_2 concentration 1200 ppm is the upper limit guideline value set by the European standard EN 15251 (2007) and the Finnish national building code for indoor air (Ministry of the Environment, Department of Built Environment, 2012).

Natural logarithms of measured CO_2 concentrations were used to calculate the outdoor air exchange rate (ACH) and evaluate the outdoor air flow rate in the ice arena (Fig. 7). The elevated night-time concentrations were used as a starting point for the (modified) decay curve calculation.

In order to use the decay method, the space had to 1) have no CO_2 sources i.e. occupant present and 2) have a constant supply air flow rate during the studied period. Only 2 periods during the measurements fulfilled the previous criteria. Based on these 2 periods, the ACH of the ice arena was found to be ~0.03 1/h. This value is much lower than values presented by Yang, Demokritou, Chen, Spengler, and Parsons (2000) which varied from 0.65 to 3.50 1/h. The outdoor air flow rate into the 13000 m^3 space can thus be estimated to be 0.108 m^3/s when the total supply air flow rate was ~2.94 m^3/s. This corresponds to an outdoor air flow fraction of 3.7 % (of supply air) which was estimated to stay constant.

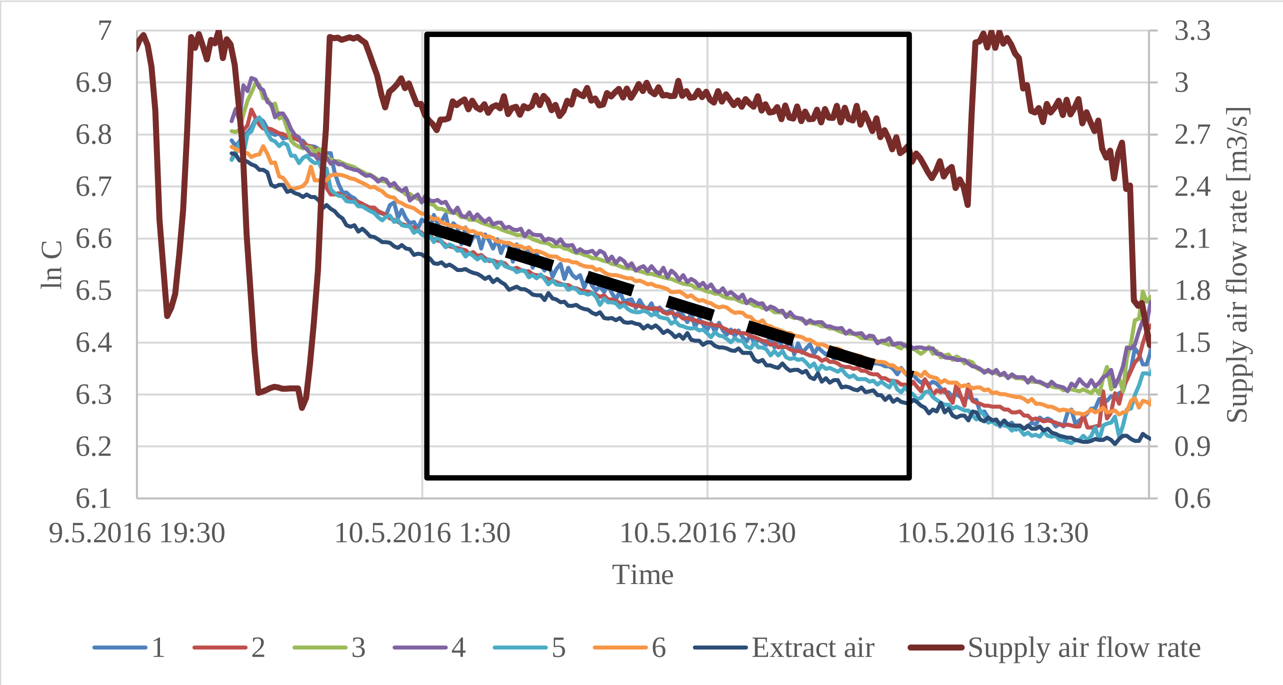

Figure 7. Decay of CO_2 concentration as a natural logarithm for air exchange rate (ACH) estimation. The rectangle represents the timeframe used for the estimation.

The supply air flow rate in the ice arena was strongly fluctuating, which was caused by the VAV ventilation system. The building automation system reacted too rapidly to changes in the occupation zone air temperature, causing unstable on-off type control of air flow rate that does not represent the best possible scenario for a VAV system. As a result, the air flow rate was either at maximum, ~3.2 m^3/s, or at minimum, ~1 m^3/s, for the majority of the measurement period.

To generate uniform conditions for the measurements on May 4th, the AHU was manually set to constant supply air flow rate of 3 m^3/s for the duration of the measurements. It should be noted that the manual control of the air flow rate influences the outcome of other measurements to some extent but is also a better representation of an average ice arena since this kind of fluctuation is not desirable.

As described in the case study presentation, only the supply air fan is operated in the AHU for the vast majority of the time. The re-circulations causes underpressure over the closed outdoor and exhaust air dampers resulting in minor outdoor air leakage of 3.7 % of supply air as calculated previously. Based on the mass balance of the entire ice arena the exfiltration through the building envelope has to be equal to the outdoor infiltration. This is consistent with the measured overpressure in the lower part of the arena. Measured pressure differences over the building envelope were mostly neutral and the average values over the envelope at occupation zone (height 2,1m) and over the roof were +1.65 Pa and -0.24 Pa respectively. The higher pressures at lower heights were caused by the (reversed) stack effect.

The temperature and relative humidity of the supply air were rapidly fluctuating, which was caused by the unoptimised performance of the building automation system. Although the setpoint of supply air temperature was 15 °C at the time of the measurements, the measured temperature varied between 11 – 31 °C with an average value of 18.8 °C. Correspondingly, the relative humidity of the supply air fluctuated between 16 – 58 % with an average value of 28 % and the absolute humidity between 2.8 – 5.5 g/kg$_{d.a.}$ with an average of 3.6 g/kg$_{d.a.}$. The fluctuation in the supply air also continued after the air flow rate was manually stabilized. Extract air temperature and relative humidity showed noticeably steadier profiles with variations between 6.2 – 16.5 °C with an average of 9.5 °C and 36 – 68 % with an average of 51 % and absolute humidity of 3.0 – 4.3 g/kg$_{d.a.}$ with an average of 3.7 g/ kg$_{d.a.}$. The rampant, i.e. clearly malfunctioning behaviour of the AHU control was not detected until the measurement day and it could not be fixed immediately on site before carrying out the measurements. Thus, the fluctuation had to be accepted and its consequent effects can be seen in the following temperature measurements.

The measured temperatures and relative humidities of the indoor air of one day are presented in Fig. 8. All temperatures were continuously fluctuating, caused by the supply air fluctuation described previously. The average temperatures at occupation zone (2m above ice) and spectator balcony over the entire measurement period were 5.3 °C and 7.1 °C respectively. Measurement points 1 and 6 constantly showed higher temperatures and less fluctuation compared to others, which was caused by the sheltered position of point 1 under the spectator balcony and the location of point 6 in the upper part of the ice arena. Fluctuation of the relative humidity followed the temperature fluctuation inversely. Manually set constant air flow rate reduced the fluctuation of temperature and relative humidity and stabilised the internal conditions.

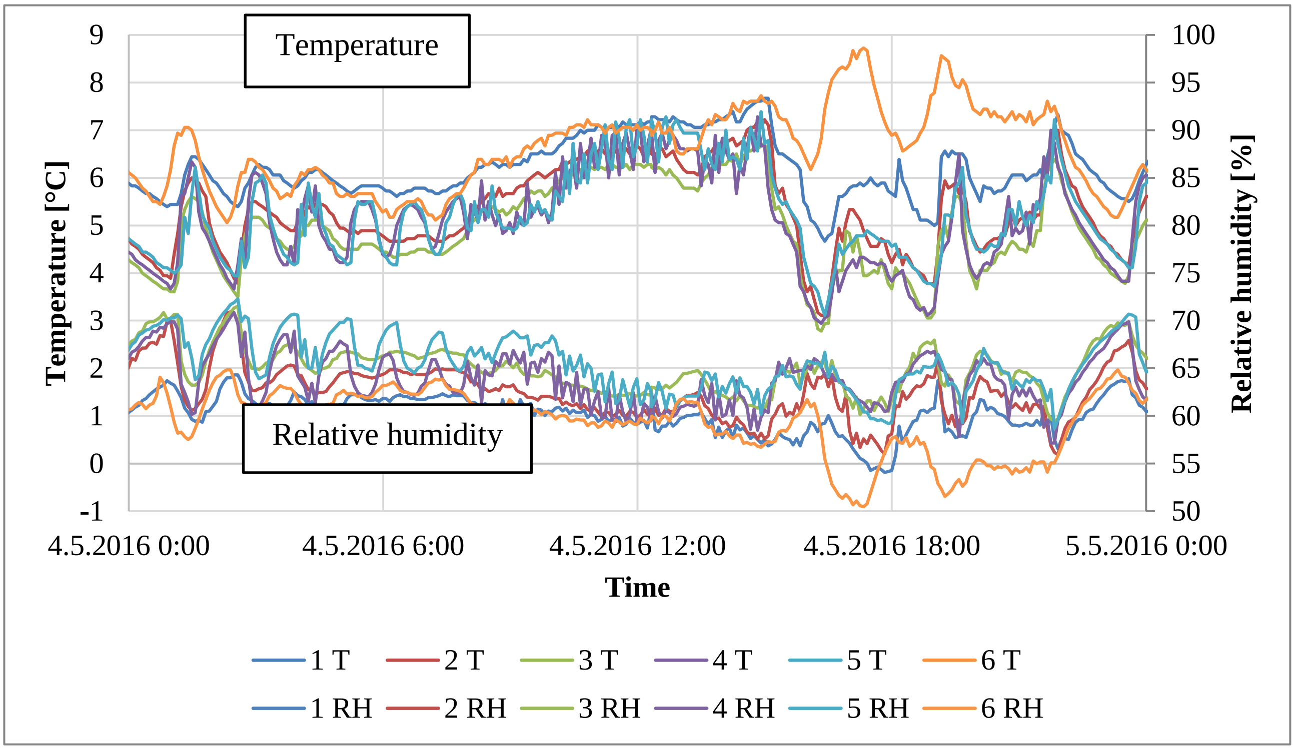

Figure 8. Measured indoor air temperatures and relative humidities of all indoor air measurement points on May 4th 2016.

Vertical gradient

Vertical gradient of room air temperature measurement results of all eight measurements points are shown in Fig. 9 along with the bolded average and the measured relative humidity average. The room air temperature gradient shows a parabolic profile with the extreme changes near the ice surface. In the well mixed upper region (above 3 m), the air temperature is rather uniform. The differences seen in the upper, mixed zone are divided so that the higher temperatures and further stratification were measured at the extract-end and lower temperatures with no further stratification at the opposite side of the arena. The relative humidity average shows a relation to the temperature curve with highest values near the ice surface. The RH value on the ice surface is not close to 100%

because the sensor was not in contact with ice. The measured relative humidity and calculated absolute humidity at height 0.25 m have been neglected due to measurement uncertainties.

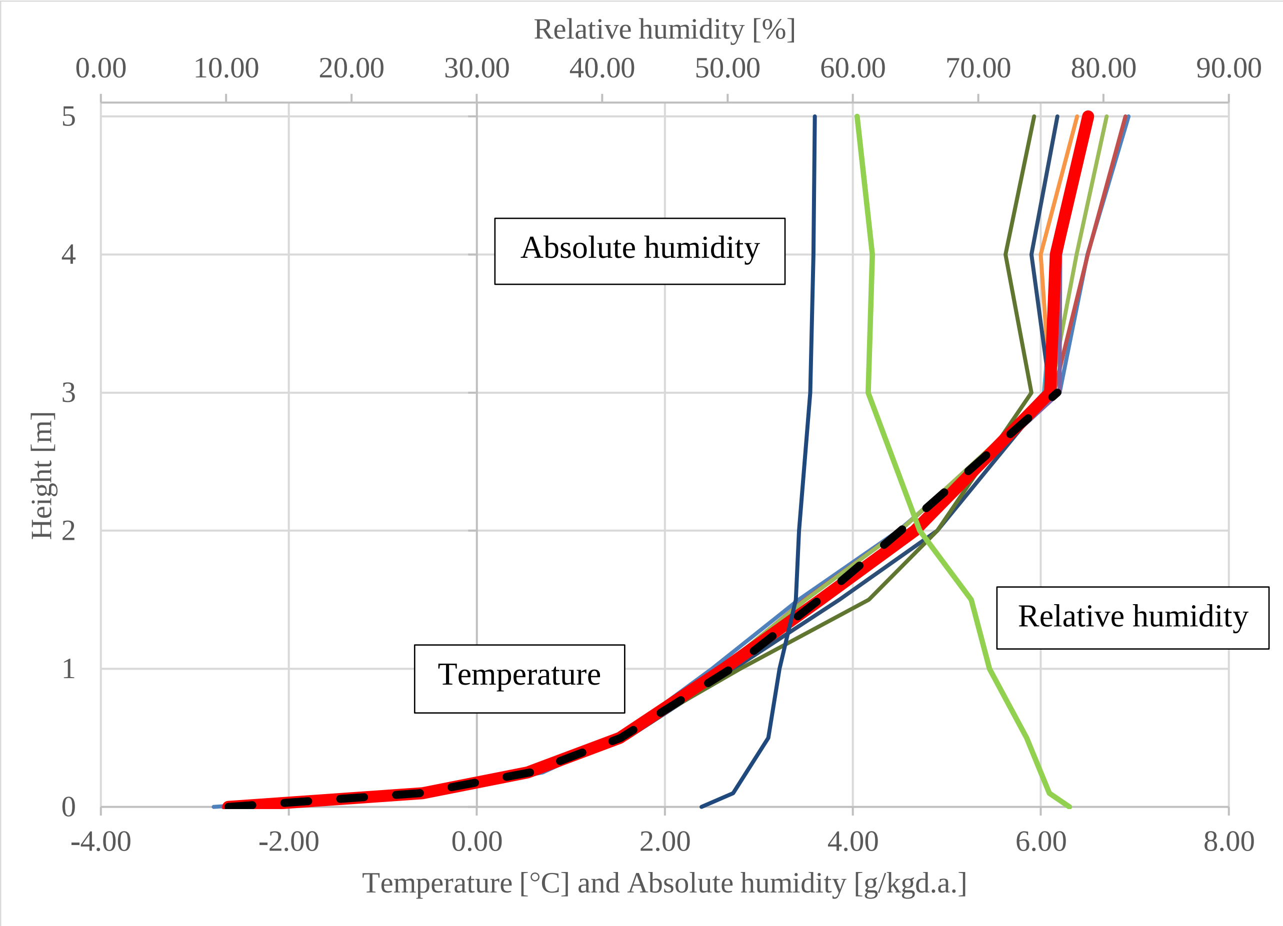

Figure 9. Measured temperature and relative humidity stratification on May 4th 2016 in the ice rink arena.

A rational fit ($R^2 = 0.9994$) for the temperature stratification from 0 to 3 meters is presented in equation (10) and plotted in Fig. 9 (dashed line).

$$T_{air} = \frac{1.584 * h^2 + 1.796 * h - 0.3349}{h + 0.1267} \quad (10)$$

Comparison of the temperature stratification results of this study to other publications is presented in Fig. 10. All measurements agree that the gradient is most severe near the ice, at heights below 1 m. Older measurements by Pennanen et al. (1997) show similar strong stratification near the ice but indicate that after the initial rise the air temperature is rather uniform which is in agreement with measurements by Yang et al. (2001) (not presented in the graph). On the other hand more recent measurements by Ouzzane et al. (2006) and Lestinen et al.(2016) show that in their cases the stratification was strong also after the initial rise which agrees with the results of this study. Measurements by Palmowska & Lipska (2016) concentrated on the lower part of the ice arenas airspace (0.1 – 1.7m) and reassure the importance of the stratification near ice level but do not address the possible stratification at higher levels. It should be noted that the different designs and layouts affecting the compared measured results are not addressed in this study.

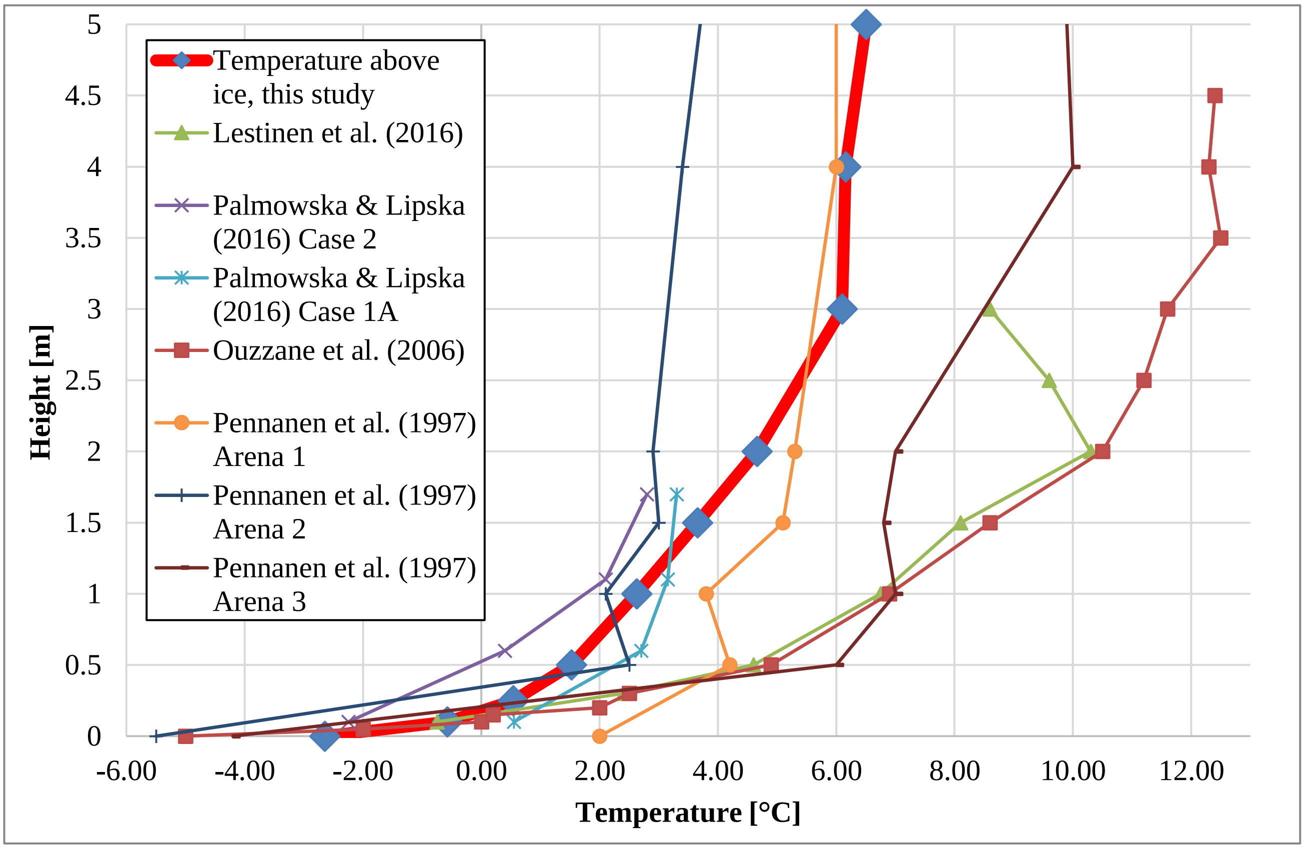

Figure 10. Vertical temperature gradient results of this study compared to other experimental results.

The results of the relative humidity (RH) above ice can be compared to two recent studies by Lestinen et al.(2016) and Palmowska & Lipska (2016). Lestinen et al.(2016) measured the RH profile to be similar to this study although the values were lower throughout the results, from 60 %

near ice level to ~47 % at the height of 2 m. On the other hand, Palmowska & Lipska (2016) presented experimental RH results that did not show a similar profile to this study and had a near uniform RH of ~90 % from the height of 0.1 to 1.7 m above ice level.

Air-exchange efficiency and mixing factor

The nominal time constant of the arena was calculated to be 33.4 h with the total volume of 13000 m^3 and outdoor air flow rate of 389 m^3/h. Air in the upper zone was assumed to be perfectly mixed at all times with mean age of air equal to the nominal time constant and air-exchange efficiency of 50 %. The results for the occupied (lower) zone are presented in Table 2.

Table 2. Mean age of air and air-exchange efficiency of the occupied zone for different mixing factor values.

β value	Occupied zone mean age of air and air-exchange efficiency
0.59	$\langle\overline{\tau}\rangle$ = 61.8h / ε_{a} = 27.1 %
1.72	$\langle\overline{\tau}\rangle$ = 43.2h / ε_{a} = 38.7 %
2.2	$\langle\overline{\tau}\rangle$ = 41.0h / ε_{a} = 40.7 %

The mixing parameter β was calculated to be 1.72 on average for the entire measurement period and found to be dependent on the air flow rate and the user activity. For this average value only the time periods when the air flow rate was above 3 m^3/s and the users were presumably on ice was considered. The users were assumed to be on ice between the time period of 16.00 – 23.00. The average mixing parameter of 1.75 was acquired for the entire measurement period when values over 20 and under 0 were neglected. The neglected values represent the situations not corresponding with the assumptions made for these calculations. Results of the mixing factor β for a one day period (May 8th 2016) are presented in Fig. 11a.

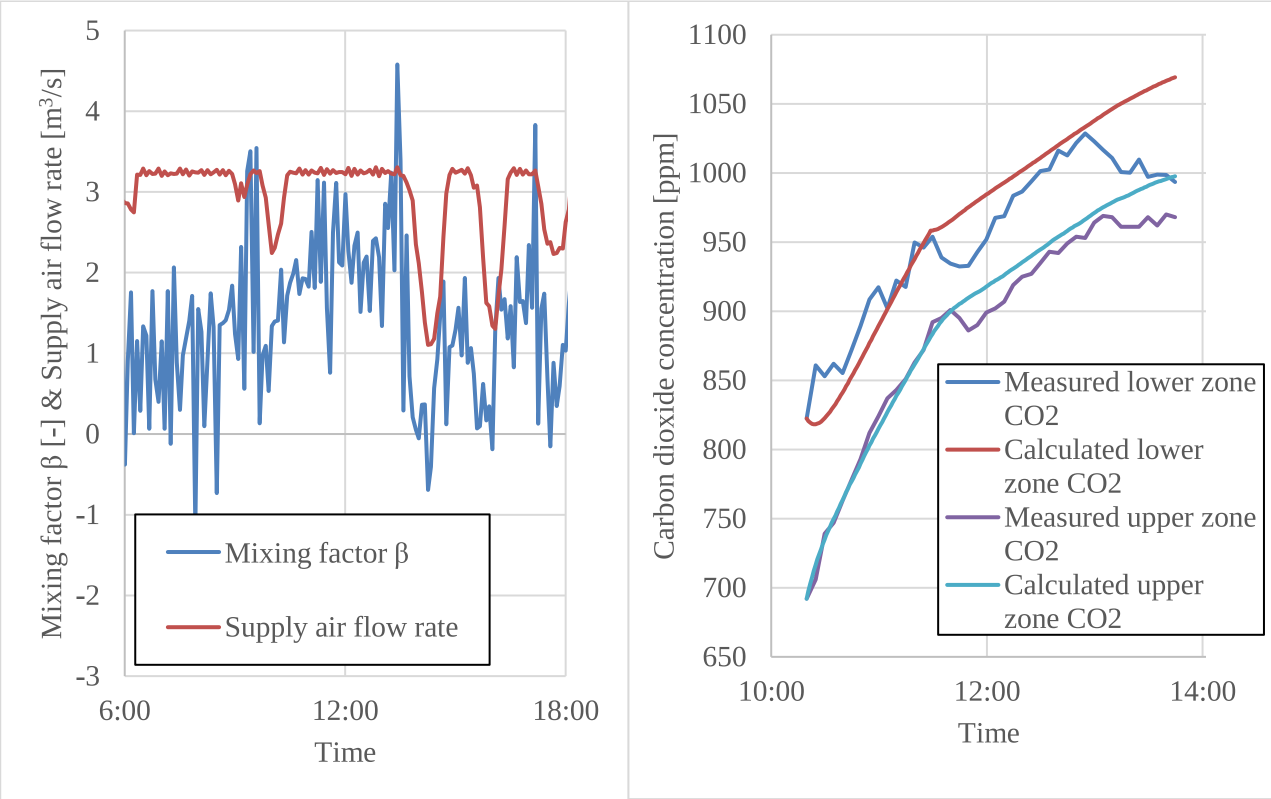

Figure 11. a) Results of the calculated mixing factor β and the measured supply air flow rate of May 8th 2016 06:00 – 18:00, b) Comparison of calculated and measured CO_2 concentrations of the upper and lower (occupation) zone.

The numerical results of the mixing parameter β were combined with a given CO_2 gain in the ice rink to evaluate the validity of the mixing parameter results. The time period of 10:20 – 13:45 on May 8th was studied as the air flow rate was measured to be constant (3.2 m^3/s) at that time (Fig. 11 a). During this period, the mixing parameter β was calculated to be 2.2 on average with standard deviation of 0.74. Two CO_2 gains of 750 & 550 $\mu m^3/s$ were introduced to represent the two different ice usage sessions during the studied timeframe. These gains correspond to 32 and 24 people with MET 5 respectively (ISO 8996, 2004). The volumes of the upper and lower (occupation) zone were set to 7500 & 5500 m^3 respectively.

The drop in the measured concentrations was caused by the ice resurfacing between the two sessions as the door for the ice maintenance machine had to be opened and outdoor air infiltration was inevitable. The fresh air intake of resurfacing was not taken into account in the calculations. The calculated concentrations with estimated contaminant sources show good agreement with measured values that are shown in Fig. 11 b. The measured CO_2 concentration of the lower zone in Fig. 11 b is the average of measurement results from points 1 to 5.

Figure 12 summarises the air distribution and stratification performance and the main results of the case-study ice arena.

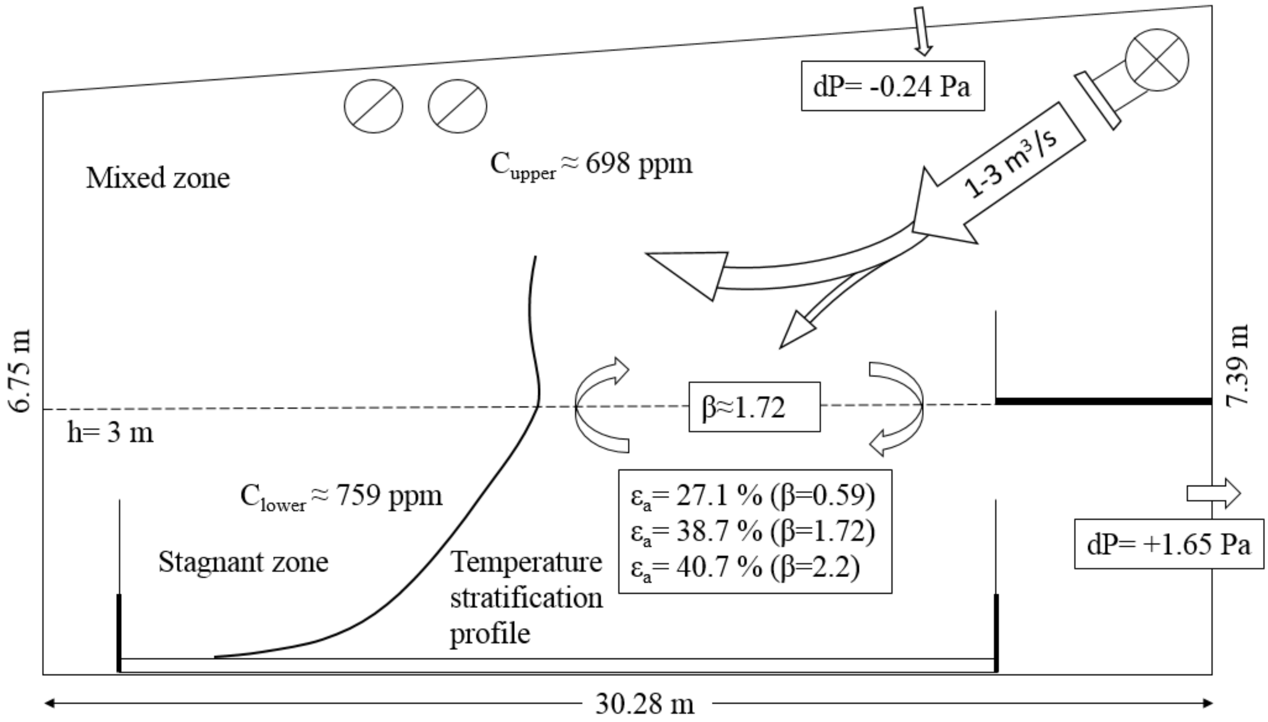

Figure 12. Schematic zones and stratification in the ice rink arena with main results.

Conclusions

Indoor ice rink arenas present challenging and unique indoor environments. In this paper, the ventilation performance and indoor air conditions of a typical Finnish ice arena were studied in order to evaluate the air change efficiency, stratification and the use of recirculation air. The air-exchange efficiency ε_a and the mixing factor β were calculated for the two incompletely mixed air zones found by smoke tests.

In the studied case, the following conclusions can be made:

- The ceiling distributed ventilation was not able to mix the ice arenas air space sufficiently and resulted in short circuiting in the upper zone.
- Two air zones were found with smoke tests: lower, stagnant occupation zone and the upper, well mixed zone.
- The stratification of air over the ice pad was measured to be substantial.
- Mixing factor β between the two zones was calculated to be 1.7 on average which indicates poor mixing of the warm supply air from the upper zone into the lower, occupied zone.
- The air-exchange efficiency ε_a for the lower zone was calculated to be 27 – 41 %, dependent on the mixing factor β, indicating less than perfect mixing in the occupation zone. The upper zone was assumed to be fully mixed (ε_a=50%).
- The ventilation was continuously operated in the re-circulation mode, which changes the current understanding about the common design assumptions.
- The outdoor air flow rate was estimated to be 3.7 % of the supply air flow rate. In normal conditions, outdoor air was taken into the system only through closed outdoor and exhaust dampers leakages and infiltration of the hall. The system was operated with outdoor air ventilation only in couple of very short time peak attendance conditions when the indoor air CO_2 concentration exceeded the setpoint of the control system. In normal operation with closed dampers the outdoor air flow rate corresponded to an air exchange rate (ACH) of 0.03 1/h.

Acknowledgements

This work was supported by the Finnish Ministry of Education and Culture under Grant OKM/105/626/2015 and L.V.Y. Foundation. The authors would like to express gratitude to Mr.

Petteri Kivivuori from the Aalto University for contributing to the measurements.

References

ASHRAE. (2013). *Handbook - Fundamentals (I-P Edition).* American Society of Heating, Refrigerating and Air-Conditioning Engineers, Inc.

Bellache, O., Galanis, N., Ouzzane, M., Sunyé, R., & Giguère, D. (2006). Two-Dimensional Transient Model of Airflow and Heat Transfer in Ice Rinks. *ASHRAE Transactions*, *2*(112), 706-716.

Bellache, O., Ouzzane, M., & Galanis, N. (2005). Coupled Conduction, Convection, Radiation Heat Transfer with Simultaneous Mass Transfer in Ice Rinks. *Numerical Heat Transfer*, 219-238.

Chen, Q., & Srebric, J. (2002). A Procedure for Verification, Validation, and Reporting of Indoor Environment CFD Analyses. *HVAC&R Research*, 201-216.

Daoud, A., Galanis, N., & Bellache, O. (2008). Calculation of refrigeration loads by convection, radiation and condensation in ice rinks using a transient 3D zonal model. *Applied Thermal Engineering*, *28*, 1782-1790.

Delta OHM S.r.L. (2017, 3 31). Retrieved from www.deltaohm.com/ver2012/download/HD21AB_HD21AB17_M_uk.pdf

Demokritou, P., Yang, C., Chen, Q., & Spengler, J. D. (2002). An experimental method for contaminant dispersal characterization in large industrial buildings for indoor air quality (IAQ) applications. *Building and Environment*, 305-312.

Etheridge, D., & Sandberg, M. (1996). *Building Ventilation: Theory and Measurement.* John Wiley & Sons Ltd.

ETI Ltd. (2017, 3 31). Retrieved from https://thermometer.co.uk/data-loggers/594-thermadata-humidity-logger-htd.html

European committee for standardization. (2007). Indoor environmental input parameters for design and assessment of energy performance of buildings addressing indoor air quality, thermal environment, lighting and acoustics. *EN 15251*.

Heiselberg, P., Murakami, S., & Roulet, C.-A. (1998). *Ventilation of Large Spaces in Buildings.* Kolding: Aalborg University.

IIHF. (2016). *Ice Rink Guide.* International Ice Hockey Federation.

ISO 8996. (2004). Ergonomics of the thermal environment - Determination of metabolic rate.

Lestinen, S., Koskela, H., Jokisalo, J., Kilpeläinen, S., & Kosonen, R. (2016). The use of displacement and zoning ventilation in a multipurpose arena. *International Journal of Ventilation, 15*(2), 151-166.

Liddament, M. W., Moser, A., Clancy, E., Collineau, S., Fortaine, J.-R. P., Howarth, A., . . . Yoshino, H. (1998). *Energy-Efficient Ventilation of Large Enclosures.* International Energy Agency.

Liu, W., Wen, J., Lin, C.-H., Liu, J., Long, Z., & Chen, Q. (2013). Evaluation of various categories of turbulence models for predicting air distribution in an airliner cabin. *Building and Environment*(65), 118-131.

Ministry of the Environment, Department of Built Environment. (2012). National Building Code of Finland D2 Indoor Climate and Ventilation of Buildings. Ministry of the Environment.

Mundt, E., Mathisen, H. M., Nielsen, P. V., & Moser, A. (2004). *Ventilation Effectiveness, Guidebook No 2.* Forssa: Rehva.

Omri, M., & Galanis, N. (2010). Prediction of 3D airflow and temperature field in an indoor ice rink with radiant heat sources. *Building Simulation*, 153-163.

Omri, M., Barrau, J., Moreau, S., & Galanis, N. (2016). Three-dimensional transient heat transfer and airflow in an indoor ice rink with radiant heat sources. *Building Simulation, 9*(2), 175-182.

Ouzzane, M., Zmeureanu, R., Scott, J., Sunyé, R., Giguère, D., & Bellache, O. (2006). Cooling Load and Environmental Measurements in a Canadian Indoor Ice Rink. *ASHRAE Transactions*, *112*, 538.

Palmowska, A., & Lipska, B. (2016). Experimental study and numerical prediction of thermal and humidity conditions in the ventilated ice rink arena. *Building and Environment*(108), 171-182.

Pennanen, S., Salonen, R. O., Aim, S., Jantunen, M. J., & Pasanen, P. (1997). Characterization of Air Quality Problems in Five Finnish Indoor Ice Arenas. *Journal of the Air & Waste Management Association*.

Rotronic AG. (2017, 24 3). *https://www.rotronic.com/en/humidity_measurement-feuchtemessung-mesure_de_l_humidite/humidity-feuchtemessung-landing-mr*. Retrieved from https://www.rotronic.com/en/cl11.html: https://www.rotronic.com/en/cl11.html

Sensor Electronic. (2017, 3 31). Retrieved from www.sensor-electronic.pl/pdf/MAN_AirDistSys5000.pdf

Swema AB. (2017, 3 24). *http://www.swema.com/*. Retrieved from Swema 3000md: http://www.swema.com/instrument.php?p=Swema%203000md van Hooff, T., & Blocken, B. (2012). Full-scale measurements of indoor environmental conditions and natural ventilation in a large semi-enclosed stadium: Possibilities and limitations for CFD validation. *Journal of Wind Engineering and Industrial Aerodynamics*, 330-341.

Yang, C., Demokritou, P., Chen, Q., & Spenger, J. (2001). Experimental Validation of a Computational Fluid Dynamics Model for IAQ Applications in Ice Rink Arenas. *Indoor Air*(11), 120-126.

Yang, C., Demokritou, P., Chen, Q., Spengler, J., & Parsons, A. (2000). Ventilation and Air Quality in Indoor Ice Skating Arenas. *ASHRAE Transactions*, 338.